In Vitro and In Vivo Evaluation of Copper-64-Octreotide Conjugates

Carolyn J. Anderson, Tammy S. Pajeau, W. Barry Edwards, Elizabeth L.C. Sherman, Buck E. Rogers and Michael J. Welch

Washington University School of Medicine, Mallinckrodt Institute of Radiology, St. Louis, Missouri

Copper-64 ($T_{1/2}$ = 12.8 hr) is a reactor-produced radionuclide that has applications in both nuclear medicine imaging by PET and radiotherapy. Octreotide, a somatostatin receptor ligand, has been conjugated with TETA and CPTA, labeled with ^{64}Cu, evaluated both in vitro and in vivo and compared to ^{111}In-DTPA-D-Phe^1-octreotide. **Methods:** The carboxylic acid moieties on theT bifunctional chelates were conjugated to the N-terminal amine of D-Phe using the linking agents hydroxybenzotriazol (HOBT) and diisopropylcarbodiimide (DIC). Receptor binding assays on all three radiolabeled octreotide conjugates were accomplished in AtT20 mouse pituitary carcinoma cell membranes. In vivo biodistribution was performed using normal Sprague-Dawley rats and Lewis rats carrying a somatostatin receptor-positive rat pancreatic tumor. **Results:** The binding affinities of ^{64}Cu-CPTA-D-Phe^1-octreotide and ^{64}Cu-TETA-D-Phe^1-octreotide in AtT20 cell membranes were both greater than ^{111}In-DTPA-D-Phe^1- octreotide (K_d, 78.5 pM, 314 pM and 3.28 nM, respectively). In normal rats, ^{64}Cu-CPTA-D-Phe^1-octreotide was localized primarily in the liver. Copper-64-TETA-D-Phe^1-octreotide, similar to ^{111}In-DTPA-D-Phe^1-octreotide, had moderate uptake in the kidneys; the hepatobiliary uptake was negligible. In rats bearing CA 20948 pancreatic tumors, both ^{64}Cu-CPTA-D-Phe^1-octreotide and ^{64}Cu-TETA-D-Phe^1-octreotide had uptake in tumors comparable to or better than ^{111}In-DTPA-D-Phe^1-octreotide. **Conclusion:** Of the two ^{64}Cu-labeled octreotide conjugates evaluated, ^{64}Cu-CPTA-D-Phe^1-octreotide has the highest affinity for the somatostatin receptor; however, the clearance was hepatobiliary with slow excretion. Copper-64-TETA-D-Phe^1-octreotide binds to the somatostatin receptor with five times the affinity of ^{111}In-octreotide, has desirable clearance properties (renal clearance with rapid excretion) and is a potential agent for PET imaging of somatostatin receptors.

Key Words: indium-111-octreotide; DTPA; copper-64-TETA octreotide; receptor binding

J Nucl Med 1995; 36:2315–2325

Somatostatin is a 14 amino acid peptide which plays an inhibitory role in the normal regulation of several organ systems: the central nervous system (CNS), the hypothalamus and the pituitary gland; the gastrointestinal tract; and the exocrine and endocrine pancreas (*1–3*). Somatostatin receptors have been demonstrated in these organ systems, and several human tumors are also somatostatin receptor-positive (*4*). The pharmacological properties of somatostatin have centered on its use for therapeutic purposes. Much of the work has centered on tumors of the neuroendocrine system (*5,6*), but other common types of tumors also contain somatostatin receptors, such as those of the CNS (*7*), breast (*8,9*) and lung (*10*). The ability to visualize somatostatin receptors in vivo for a large number of different tumor types using nuclear medicine will have a great effect on the biological characterization of cancers. Furthermore, the presence of somatostatin receptors in a tumor is predictive of a good therapeutic response.

Somatostatin is unsuitable for in vivo use due to its short biological half-life. Octreotide, an eight amino acid peptide, is an analog of somatostatin that is highly resistent to degradation by enzyme attack and is longer acting than the native somatostatin (*11*). Octreotide is also 2000 times more effective than somatostatin in the suppression of growth hormone secretion in the rat 1 hr postinjection (*11*).

Octreotide has been labeled with ^{123}I (*12*) and ^{111}In (*13*) and used to image somatostatin receptor-positive tumors in humans (*14,15*). Iodine-123-Tyr-3-octreotide had a high hepatobiliary excretion which hinders visualization of tumors in the abdomen, whereas ^{111}In-DTPA-D-Phe^1-octreotide clears primarily through the kidneys (*16*). Although the blood clearance of the ^{111}In-labeled peptide was considerably slower than that of ^{123}I-Tyr^3-octreotide, because ^{111}In-labeled DTPA-D-Phe^1-octreotide remains intact in vivo, the background radioactivity in the body is much lower than that of the iodinated peptide, making ^{111}In-DTPA-D-Phe^1-octreotide more sensitive for imaging certain types of tumors (*15*).

Because it is difficult to quantify images by SPECT, SPECT imaging with either ^{123}I- or ^{111}In-labeled octreotide allows only a qualitative or, at most, a rough quantitative estimate of the number of somatostatin receptors on tumors. By using octreotide labeled with a positron-emitting radionuclide and PET, quantitative assessment of tracer accumulation within tissues would be achievable. This offers marked improvements over gamma camera imaging,

Received Nov. 10, 1994; revision accepted Feb. 14, 1995.

For correspondence or reprints contact: Carolyn J. Anderson, PhD, Mallinckrodt Institute of Radiology, 510 S. Kingshighway Blvd., Box 8225, St. Louis, MO 63110.

especially for tumor deposits deep within the body or for small tumor deposits such as metastatic cancer within lymph nodes. PET imaging with a radiolabeled somatostatin receptor ligand will allow quantitation of the number of somatostatin receptors and therefore will be useful in predicting the eventual clinical response of patients who will then undergo therapy with octreotide.

Octreotide has been conjugated to desferrioxamine (DFO), labeled with the positron-emitting radionuclide ^{68}Ga ($T_{1/2}$ = 68 min) and investigated in vitro and in tumor-bearing rats (*17*). The biodistribution of ^{68}Ga-DFO-octreotide is similar to that of ^{111}In-DTPA-D-Phe^1-octreotide. Since the background radioactivity in humans injected with ^{111}In-DTPA-D-Phe^1-octreotide was significantly lower at 24 hr compared to 4 hr postinjection, resulting in superior images in patients (*17*), ^{68}Ga may not be an ideal radionuclide for labeling octreotide. Octreotide has also been labeled with ^{18}F ($T_{1/2}$ = 110 min) and biodistribution was determined in nontumor-bearing mice (*18*). This compound is cleared primarily through the hepatobiliary system and may suffer the same problems as iodinated octreotide for imaging. An alternative metal radionuclide for PET imaging is ^{64}Cu. Copper-64 [$T_{1/2}$ = 12.8 hr; electron capture (41%); β^- (0.573 MeV, 40%); β^+ (0.656 MeV, 19%); γ (0.511 MeV, 38%, 1.34 MeV, 0.5%)] is produced in high specific activity (>960 GBq/mmol (26,000 Ci/mmol)) at the University of Missouri Research Reactor. It has been demonstrated that ^{64}Cu-labeled radiopharmaceuticals give satisfactory PET images 24-hr postinjection (*19*). PET imaging of tumors using low doses of ^{64}Cu-labeled-octreotide could also be utilized to determine individual radiation dosimetry prior to therapy with either ^{64}Cu- or ^{67}Cu-labeled octreotide. For these reasons, we are investigating the development of a ^{64}Cu-labeled octreotide conjugate for PET imaging.

In this study, we synthesized two new octreotide conjugates, TETA-D-Phe^1-octreotide and CPTA-D-Phe^1-octreotide for radiolabeling with ^{64}Cu (in which TETA is 1,4,8,11-tetraazacyclotetradecane-N,N′,N″,N‴ tetraacetic acid and CPTA is 4-[1,4,8,11-tetraazacyclotetradec-1-ylmethyl] benzoic acid) (Fig. 1). In vitro binding affinity of the ^{64}Cu-labeled octreotide conjugates for the somatostatin receptor was determined in AtT20 mouse pituitary carcinoma cell membranes. In vivo receptor binding was determined in normal Sprague-Dawley rats, using the adrenal gland as a target organ, and in somatostatin receptor-positive tumors in Lewis rats. Rat adrenal glands are known to have a high concentration of somatostatin receptors (*20,21*). The receptor binding and biodistribution of the ^{64}Cu-labeled octreotide conjugates were compared to that of ^{111}In-DTPA-D-Phe^1-octreotide.

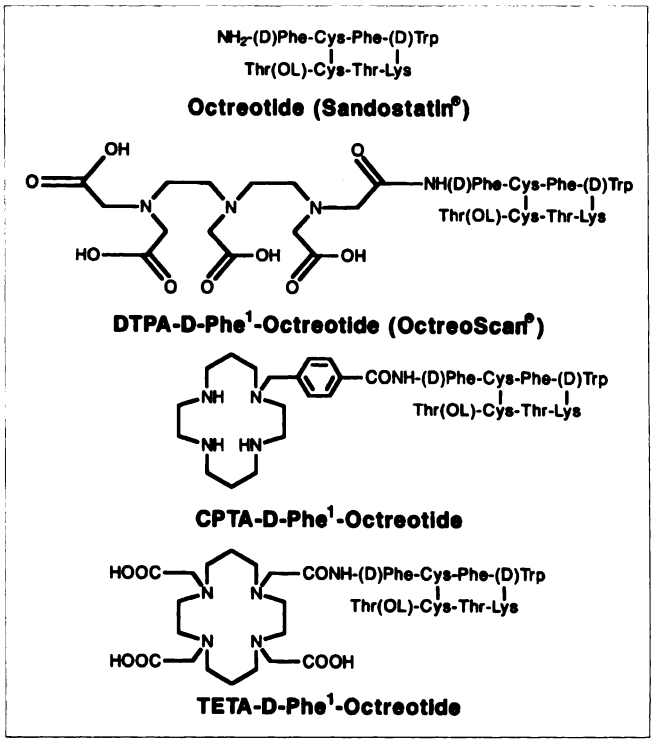

FIGURE 1. Octreotide and octreotide analogs investigated in this study.

MATERIALS AND METHODS

All chemicals were purchased from Aldrich (Milwaukee, WI) unless specified otherwise. Octreotide was purchased from DePaul Radiopharmaceutical (St. Louis, MO). Ultrapure sodium acetate was obtained from Johnson Matthey (Ward Hill, MA). Copper-64-Cl_2 (specific activity, 960–4800 GBq/mmol (26,000–130,000 Ci/mmol)) was obtained from the University of Missouri Research Reactor, and $^{111}InCl_3$ (specific activity 1720 GBq/mmol (46,500 Ci/mmol)) was obtained from Mallinckrodt Medical, Inc. (St. Louis, MO). All solutions were made using distilled deionized water (Milli-Q®; > 18 MΩ resistivity). Reversed-phase high pressure liquid chromatography (RP-HPLC) was performed on a Waters 600E chromatography system with a Waters 484 UV-absorbance detector and a Spectra Physics Chromjet integrator. RP-HPLC columns were either Vydac 218TP54 (C18, 4.6 × 250 mm), Vydac 218TP1010 (C18, 10 × 250 mm) or POROS R2/H (C8, 4.6 × 100 mm). The mobile phase was H_2O [0.1% trifluoroacetic acid (TFA)] and acetonitrile (0.1% TFA). Electrospray mass-spectrometry (ES-MS) was performed on a Vestec 201 mass spectrometer. Adult, female, Sprague-Dawley rats were purchased from Sasco (Omaha, NE) and 6–8-wk-old Lewis rats were purchased from Charles River Laboratories (Boston, MA). The rat pancreatic tumor CA20948 was obtained from the Tumor Bank at Biomeasure, Inc. (Hopkinton, MA).

Synthesis of TETA-D-Phe^1-Octreotide and CPTA-D-Phe^1-Octreotide

The chelate TETA was commercially available. CPTA was synthesized by the one-step procedure of Studer and Kaden (*22*) and was characterized by mass spectrometry, ^{1}H-NMR and elemental analysis. In the conjugation of both TETA and CPTA to octreotide (Fig. 2), the Lys residue on octreotide was protected with a Boc group by reaction with $(Boc)_2O$ in DMSO. The N-terminal amine of the Boc-protected octreotide was conjugated to one of the carboxylates on TETA and the carboxylic acid on CPTA with diisopropylcarbodiimide (DIC) in DMF using hydroxybenzotriazole (HOBT) as a catalyst. CPTA-D-Phe^1-octreotide was also synthesized using protected octreotide prepared by a solid-phase

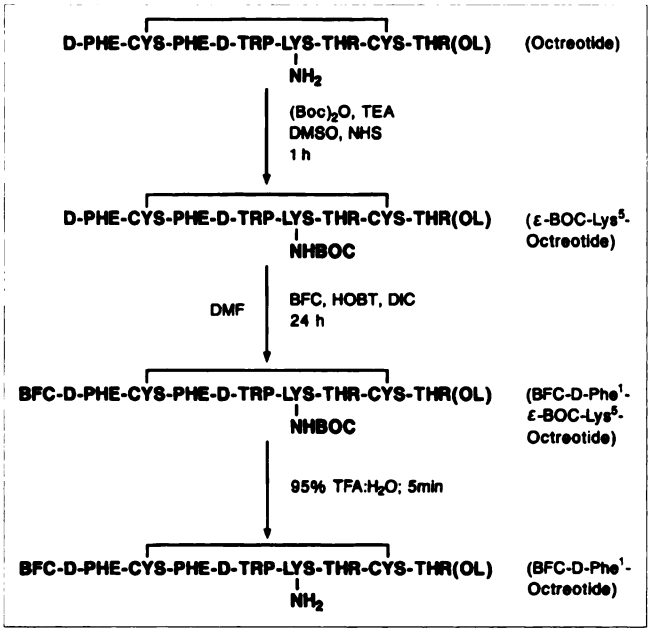

FIGURE 2. Reaction scheme for the synthesis of the two bifunctional chelate-octreotide analogs used in this study. BFC = the bifunctional chelates TETA and CPTA.

method as previously described (*23*). The specific chromatography conditions were carried out as previously described (*23*). Briefly, the reactions were monitored on Vydac 218TP54 and the major product collected by semi-preparative RP-HPLC on Vydac 218TP1010. The mobile phase was H_2O (0.1% TFA) and acetonitrile (0.1% TFA). The products, TETA-D-Phe^1-octreotide and CPTA-D-Phe^1-octreotide were characterized by electrospray mass spectrometry and purity was assessed by RP-HPLC.

Preparation of Copper-64 and Indium-111 Octreotide Conjugates

Copper-64-acetate was labeled to 1–10 μg of either TETA-D-Phe^1-octreotide or CPTA-D-Phe^1-octreotide in 0.1 *M* ammonium acetate buffer, pH 5.5. One milligram of gentisic acid per milliliter was added to the radiolabeled conjugates to reduce the effects of radiolysis. Radiochemical purity was determined by RP-HPLC. Preparations that were <95% pure were purified by a C-18 SepPak®. The ^{64}Cu-labeled octreotide conjugate was loaded onto a C-18 SepPak Light® and the SepPak® was washed with 5 ml 0.1 *M* ammonium acetate, pH 5.5, to removed unlabeled ^{64}Cu-acetate from the SepPak® while the ^{64}Cu-labeled octreotide conjugate remained. The ^{64}Cu-labeled octreotide conjugate was then eluted from the SepPak® in ethanol.

Indium-111-DTPA-D-Phe^1-octreotide was prepared using a commercial kit containing 10 μg DTPA-D-Phe^1-octreotide lyophilized in citrate buffer and gentisic acid. One milliliter $^{111}InCl_3$ in 0.02 *M* HCl was added to the kit and the mixture was incubated at room temperature for 1 hr. The product was purified using a C-18 SepPak®. DTPA-D-Phe^1-octreotide prepared by solid-phase peptide synthesis (*23*) was also labeled with ^{111}In-citrate in 0.1 *M* ammonium citrate, pH 5.5, and gentisic acid. This product was purified as previously described. Radiochemical purity was assesed by RP-HPLC on POROS R2/H.

In Vitro Studies

The binding characteristics of ^{64}Cu-TETA-D-Phe^1-octreotide, ^{64}Cu-CPTA-D-Phe^1-octreotide and ^{111}In-DTPA-D-Phe^1-octreotide have been investigated in AtT20 cells. A preparation of cell membranes was made from AtT20 cells by brief sonication followed by centrifugation at 13,000 rpm. The membranes were resuspended in a HEPES buffer containing 0.1% BSA and 1 mg/ml aprotinin (*24*).

Experiments were performed to obtain data for Scatchard analysis. Equal volumes of membranes were added to varying concentrations of tracer (±1000-fold excess of octreotide as a blocker) in triplicate ranging over a concentration range of two orders of magnitude. Samples were incubated for 2 hr at 25°C and then centrifuged to separate the pellet from the buffer. The pellet was washed twice and both fractions were counted. The data were plotted as nanomolar tracer specifically bound versus the specific bound-to-free ratio and the dissociation constants (K_D's) and number of receptors (B_{max}) were determined along with their errors using the computer program LIGAND (*25*).

Animal Biodistribution Studies

All animal experiments were conducted in compliance with the Guidelines for the Care and Use of Research Animals established by Washington University's Animal Studies Committee.

Biodistribution experiments of injected radiolabeled octreotide conjugates were performed in normal, female Sprague-Dawley rats (140–160 g) and male Lewis rats (220–260 g) bearing the somatostatin receptor-positive rat pancreatic tumor CA20948, which has been used to evaluate other radiolabeled somatostatin analogs (*26*). In both animal models, rats anesthetized with methoxyflurane were injected intravenously with 0.55–1.7 MBq (15–45 μCi, 8–20 ng) of ^{64}Cu-CPTA-D-Phe^1-octreotide or ^{64}Cu-TETA-D-Phe^1-octreotide or 0.19–0.63 MBq (5–17 μCi, 5–113 ng) of ^{111}In-DPTA-D-Phe^1-octreotide and killed by halothane overdose at time points ranging from 1 to 36 hr postinjection. The tumor (Lewis rats), blood, lung, liver, spleen, kidney, bladder, muscle, heart, bone, adrenals, pancreas, stomach and intestines were removed, weighed and the activity counted on a gamma counter. The percent injected dose per gram (%ID/g) and percent injected dose per organ (%ID/organ) for each tissue and organ were calculated. In certain groups of rats, 250 μg (tumor-bearing Lewis rats) of octreotide were coinjected with the radiolabeled octreotide conjugate and the rats were killed 1 hr postinjection. Student t-tests were performed to determine significance of differences between biodistribution experiments.

In separate experiments, 8–10 rats were placed in metabolism cages. Sprague-Dawley rats were injected with ~3.7 MBq (100 μCi; 100 ng) ^{64}Cu-TETA-D-Phe^1-octreotide or ^{64}Cu-CPTA-D-Phe^1-octreotide. Urine and feces were collected at times ranging from 1 to 24 hr, and their activity was counted on a gamma counter. The percent injected dose for each sample was calculated.

RESULTS

Preparation of Octreotide Conjugates

The synthesis scheme of TETA-D-Phe^1-octreotide and CPTA-D-Phe^1-octreotide is shown in Figure 2. TETA-D-Phe^1-octreotide was obtained in >99% purity in 4% overall yield. ES-MS calculated: 1433 Da, experimental: 1433.75 Da. CPTA-D-Phe^1-octreotide was obtained in >99% purity in 4% overall yield. ES-MS calculated: 1335 Da, experimental: 1336 Da.

Radiolabeling Studies

Copper-64-TETA-D-Phe^1-octreotide and ^{64}Cu-CPTA-D-Phe^1-octreotide have been prepared in high specific ac-

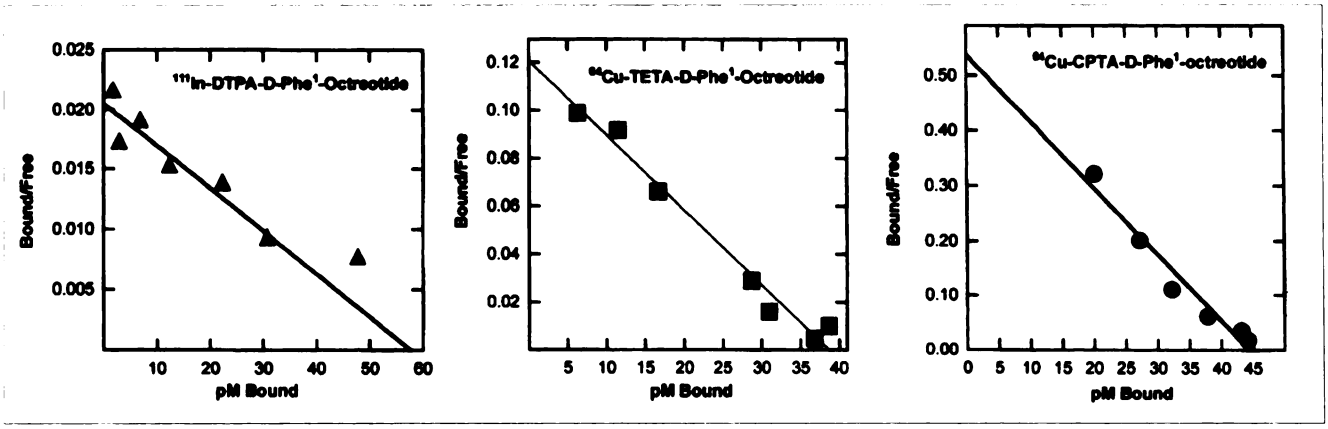

FIGURE 3. Scatchard plots for somatostatin receptor binding of ^{64}Cu-TETA-D-Phe^1-octreotide, ^{64}Cu-CPTA-D-Phe^1-octreotide and ^{111}In-DTPA-D-Phe^1-octreotide in AtT20 mouse pituitary carcinoma cell membranes. The K_d and B_{max} values for each compound are listed in Table 1.

tivity and purity suitable for future clinical studies. Specific activities for the ^{64}Cu-labeled conjugates ranged from 56 to 111 GBq/mmol (1500–3000 Ci/mmol). Typically, ^{64}Cu-acetate was incorporated into TETA-D-Phe^1-octreotide in >95% yield within 60 min postinjection and no SepPak® purification was required; however, CPTA-D-Phe^1-octreotide incorporated ^{64}CuOAc more slowly, and even after a 12–18-hr incubation, the conjugate was only 85% radiolabeled. Addition of gentisic acid was necessary to protect the conjugates against radiolysis. Both ^{64}Cu-labeled octreotide conjugates were susceptible to radiolysis, a phenomenon similar to ^{111}In-DTPA-D-Phe^1-octreotide (*13*). The radiolysis products of both ^{64}Cu-octreotide conjugates were numerous; these compounds eluted later than the void volume, but no attempt was made to identify them. Without gentisic acid, HPLC profile showed an array of radiolysis products (approximately 30% of the total integrated area) other than the radiolabeled octreotide to be present, whereas, with the addition of gentisic acid, both ^{64}Cu-labeled octreotide analogs were consistently >95% pure. Also, in the presence of gentisic acid, both ^{64}Cu-labeled octreotide conjugates remained >95% intact for at least 48 hr.

The specific activities of both commercial octreotide and ^{111}In-DTPA-D-Phe^1-octreotide labeled with the conjugate prepared in-house were 26–56 GBq/mmol (700–1500 Ci/mmol). Incorporation of $^{111}InCl_3$ into DTPA-D-Phe^1-octreotide was generally complete after 60 min. The need for SepPak® purification was dependent on the age of the $^{111}InCl_3$. Generally, purification of ^{111}In-DTPA-D-Phe^1-octreotide was not necessary unless the $^{111}InCl_3$ had decayed more than two half-lives, which thereby decreased its specific activity. HPLC analyses indicated all preparations of ^{111}In-DTPA-D-Phe^1-octreotide had >95% purity.

In Vitro Studies

To characterize the receptor binding properties of the ^{64}Cu-labeled octreotide analogs, Scatchard analysis was performed. The binding affinities of ^{64}Cu-TETA-D-Phe^1-octreotide, ^{64}Cu-CPTA-D-Phe^1-octreotide and ^{111}In-DTPA-D-Phe^1-octreotide were evaluated using mouse anterior pituitary adenoma AtT20 cells. AtT20 cells contain a high concentration of somatostatin receptors (*27*) and have been used extensively in the study of somatostatin receptor binding and in the characterization of the receptor itself (*28*). Figure 3 shows the Scatchard plots for ^{64}Cu-TETA-D-Phe^1-octreotide, ^{64}Cu-CPTA-D-Phe^1-octreotide and ^{111}In-DTPA-D-Phe^1-octreotide. Table 1 lists the dissociation constants (K_d) and number of receptors (B_{max}) for each analog in AtT20 membranes. The single K_d observed and the similar binding capacity (B_{max}) for each compound indicate a single binding site on the somatostatin receptor. At low ligand concentrations (<0.2 n*M* added), nonspecific binding for ^{111}In-DTPA-D-Phe^1-octreotide was ~30%, whereas for ^{64}Cu-CPTA-D-Phe^1-octreotide and ^{64}Cu-TETA-D-Phe^1-octreotide, it was 5%–10%. Scatchard analysis indicates ^{64}Cu-CPTA-D-Phe^1-octreotide bound to the somatostatin receptor with affinity over 40 times greater (K_d = 78.5 pM) than that of ^{111}In-DTPA-D-Phe^1-octreotide (K_d = 3.28 n*M*). Copper-64-TETA-D-Phe^1-octreotide had a K_d of 314 p*M* which indicated a binding affinity of more than 10 times that of ^{111}In-DTPA-D-Phe^1-octreotide.

TABLE 1
Dissociation Constants and Number of Receptors for Radiolabeled Octreotide Analogs in AtT20 Mouse Pituitary Cell Membranes

Octreotide analog	K_D	B_{max} (fmole/mg protein)
^{64}Cu-TETA-D-Phe^1-octreotide	314 p*M* (33%)	153 (18%)
^{64}Cu-CPTA-D-Phe^1-octreotide	78.5 p*M* (31%)	173 (11%)
^{111}In-DPTA-D-Phe^1-octreotide	3.28 n*M* (53%)	160 (44%)

The percent error calculated from LIGAND is denoted in parentheses.

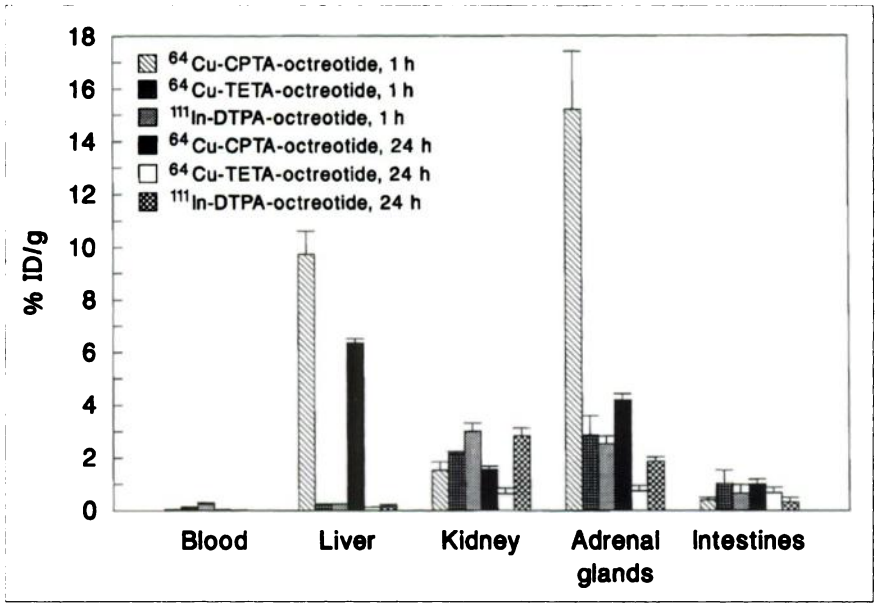

FIGURE 4. Biodistribution of ^{64}Cu-TETA-D-Phe^{1}-octreotide, ^{64}Cu-CPTA-D-Phe^{1}-octreotide and ^{111}In-DTPA-D-Phe^{1}-octreotide in normal Sprague-Dawley rats at 1 and 24 hr postinjection (n = 4).

Animal Biodistribution Studies

Biodistribution of the ^{64}Cu-labeled octreotide analogs compared to ^{111}In-DTPA-octreotide is shown in Figure 4. The uptake of ^{64}Cu-CPTA-D-Phe^{1}-octreotide in the adrenal glands 1 hr postinjection (15.2% ± 2.2% ID/g) was approximately five times greater than that of either ^{64}Cu-TETA-D-Phe^{1}-octreotide (2.9% ± 0.7% ID/g) or ^{111}In-DTPA-D-Phe^{1}-octreotide (2.5% ± 0.3% ID/g); however, the liver uptake of ^{64}Cu-CPTA-D-Phe^{1}-octreotide (9.7 ± 0.9 %ID/g) at this time was nearly 40 times greater than the other compounds, and it did not clear notably by 24 hr (6.4% ± 0.2 %ID/g). The blood clearance was rapid for all three compounds; the half-life of the three compounds in the blood ranged from 8 to 10 min (Fig. 5). The kidney clearance in rats from 1 to 24 hr postinjection of all three radiolabeled analogs is shown in Figure 6. Indium-111-DTPA-D-Phe^{1}-octreotide had a significantly higher uptake in the kidneys at times up to 24 hr postinjection than either of the ^{64}Cu-labeled analogs ($p < 0.002$). Only ^{64}Cu-TETA-D-Phe^{1}-octreotide appears to clear appreciably from the kidneys (0.66% ± 0.21 %ID/g at 24 hr).

Biodistribution experiments were also accomplished in Lewis rats bearing CA20948 rat pancreatic tumors (Tables 2 and 3). The biodistribution of all three radiolabeled oct-

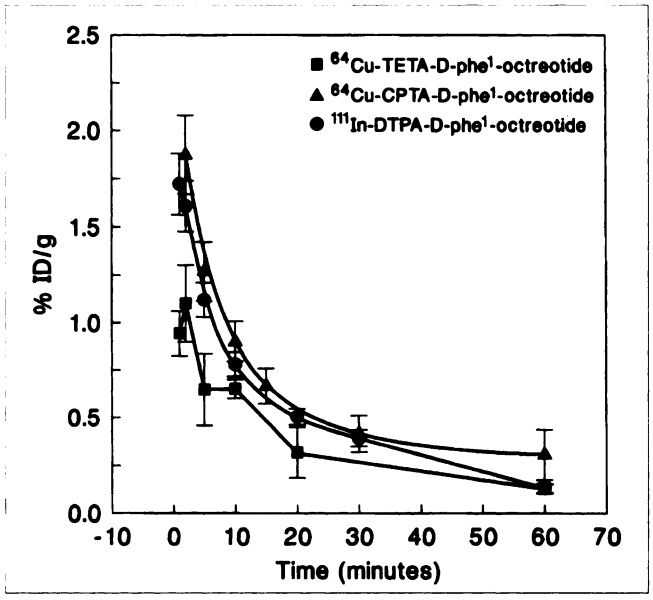

FIGURE 5. Blood clearances in normal Sprague-Dawley rats out to 60 min postinjection of ^{64}Cu-TETA-D-Phe^{1}-octreotide, ^{64}Cu-CPTA-D-Phe^{1}-octreotide and ^{111}In-DTPA-D-Phe^{1}-octreotide (n = 4).

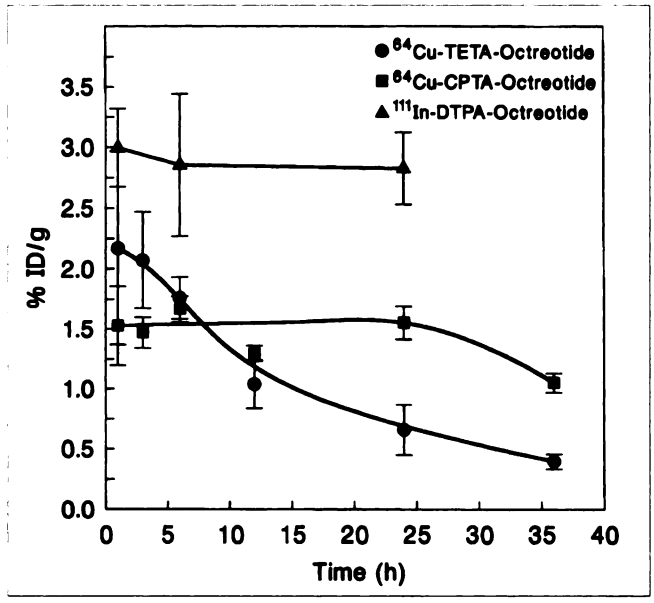

FIGURE 6. Kidney clearances in normal Sprague-Dawley rats out to 36 hr postinjection of ^{64}Cu-TETA-D-Phe^{1}-octreotide, ^{64}Cu-CPTA-D-Phe^{1}-octreotide and ^{111}In-DTPA-D-Phe^{1}-octreotide (n = 4).

TABLE 2
Biodistribution (%ID/g ± s.d.) at 1 and 24 Hours Postinjection of Copper-64-TETA-Octreotide, Copper-64-CPTA-Octreotide and Indium-111-DTPA-Octreotide in Lewis Rats Bearing CA20948 Rat Pancreatic Tumors

Tissue	^{64}Cu-TETA-Oct 1 hr (n = 4)	^{64}Cu-CPTA-Oct 1 hr (n = 4)	^{111}In-DTPA-Oct 1 hr (n = 4)	^{64}Cu-TETA-Oct 24 hr (n = 4)	^{64}Cu-CPTA-Oct 24 hr (n = 3)	^{111}In-DTPA-Oct 24 hr (n = 3)
Blood	0.13 ± 0.025	0.17 ± 0.030	0.13 ± 0.009	0.058 ± 0.02	0.09 ± 0.008	0.003 ± 0.001
Liver	0.23 ± 0.010	6.60 ± 0.20	0.13 ± 0.01	0.21 ± 0.02	3.86 ± 0.41	0.039 ± 0.001
Spleen	0.065 ± 0.02	2.05 ± 0.38	0.063 ± 0.01	0.07 ± 0.02	0.60 ± 0.078	0.03 ± 0.002
Kidney	2.18 ± 0.25	1.99 ± 0.24	3.18 ± 0.24	0.65 ± 011	1.65 ± 0.31	3.04 ± 0.12
Muscle	0.04 ± 0.007	0.04 ± 0.004	0.04 ± 0.003	0.01 ± 0.001	0.02 ± 0.004	0.004 ± 0.001
Adrenals	2.86 ± 0.29	16.9 ± 1.44	1.11 ± 0.22	1.00 ± 0.16	6.52 ± 0.85	0.69 ± 0.18
Pancreas	0.86 ± 0.14	0.59 ± 0.043	0.42 ± 0.09	0.25 ± 0.04	0.24 ± 0.03	0.20 ± 0.02
Intestines	0.13 ± 0.02	0.18 ± 0.01	0.15 ± 0.05	0.18 ± 0.012	0.30 ± 0.04	0.067 ± 0.02
Tumor	0.91 ± 0.23	0.69 ± 0.07	0.57 ± 0.10	0.24 ± 0.04	0.19 ± 0.04	0.32 ± 0.005
Tumor/Blood	7.10 ± 1.29	4.20 ± 0.53	4.48 ± 0.66	4.41 ± 1.29	2.18 ± 0.51	87.0 ± 20.1
Tumor/Muscle	25.0 ± 2.01	16.6 ± 1.28	15.5 ± 2.82	27.7 ± 2.55	8.03 ± 1.05	68.6 ± 22.3
Tumor/Liver	7.06 ± 0.80	0.10 ± 0.01	4.34 ± 0.50	1.16 ± 0.19	0.05 ± 0.01	6.59 ± 0.58

reotide analogs was similar to that in normal Sprague-Dawley rats. The tumor uptake of both ^{64}Cu-TETA-D-Phe^1-octreotide and ^{64}Cu-CPTA-D-Phe^1-octreotide at 1 hr postinjection was significantly greater than that of ^{111}In-DTPA-D-Phe^1-octreotide ($p < 0.04$); however, the tumor uptake of ^{111}In-DTPA-D-Phe^1-octreotide was significantly higher than that of both ^{64}Cu-labeled octreotide conjugates at 24 hr postinjection ($p < 0.02$). At 1 hr postinjection, all tumor-to-nontarget organ ratios are greater for ^{64}Cu-TETA-D-Phe^1-octreotide than both ^{64}Cu-CPTA-D-Phe^1-octreotide or ^{111}In-DTPA-D-Phe^1-octreotide; however, by 24 hr they are significantly higher for ^{111}In-DTPA-D-Phe^1-octreotide. For all three radiolabeled octreotide analogs, the uptake in the tumor was significantly less at 1 hr postinjection in the rats that received the co-injected blocking dose ($p < 0.002$).

For nearly all time points, the tumor uptake of ^{64}Cu-CPTA-D-Phe^1-octreotide was not significantly different than that of ^{64}Cu-TETA-D-Phe^1-octreotide and similar to or less than ^{111}In-DTPA-D-Phe^1-octreotide; however, ^{64}Cu-CPTA-D-Phe^1-octreotide had an uptake in the adrenals more than 5 times that of ^{64}Cu-TETA-D-Phe^1-octreotide and more than 15 times that of ^{111}In-DTPA-D-Phe^1-octreotide. This was similar to the biodistributions of the radiolabeled octreotide analogs in normal Sprague-Dawley rats. In tumor-bearing rats at 1 hr postinjection, the pancreatic uptake of ^{64}Cu-CPTA-D-Phe^1-octreotide is less than that of ^{64}Cu-TETA-D-Phe^1-octreotide ($p < 0.03$) but greater than that of ^{111}In-DTPA-D-Phe^1-octreotide ($p < 0.05$). By 24 hr postinjection, however, the pancreatic uptake is not significantly different between all three octreotide analogs. At 1 hr postinjection, the differences in pancreatic uptake between the radiolabeled octreotide analogs were much less than the differences in adrenal uptake.

The excretion data of ^{64}Cu-TETA-D-Phe^1-octreotide and ^{64}Cu-CPTA-D-Phe^1-octreotide in rats is shown in Table 4. More than 50% of ^{64}Cu-TETA-D-Phe^1-octreotide was excreted into the urine by 1 hr postinjection, whereas ~6% of the injected ^{64}Cu-CPTA-D-Phe^1-octreotide was excreted by 1 hr. By 24 hr postinjection ~80% of radioactivity from ^{64}Cu-TETA-D-Phe^1-octreotide was found in the urine and feces while ~40% of ^{64}Cu-CPTA-D-Phe^1-octreotide activity was excreted. The total fecal activity for both ^{64}Cu-labeled octreotide conjugates was <10% ID/g by 24 hr postinjection.

DISCUSSION

One of the goals in this project is to develop a PET agent for imaging somatostatin receptor-positive tumors in humans. Copper-64, a positron-emitting radionuclide with a half-life of 12.8 hr, has been used to label monoclonal antibodies (MAb 1A3) for imaging of colorectal cancer and

TABLE 3
Uptake of Copper-64-TETA-Octreotide, Copper-64-CPTA-Octreotide and Indium-111-DTPA-Octreotide in Somatostatin Receptor-Positive Tumors and Organs 1 Hour Postinjection

Tissue	^{64}Cu-TETA-Oct 1 hr	^{64}Cu-TETA-Oct 1 hr block	^{64}Cu-CPTA-Oct 1 hr	^{64}Cu-CPTA-Oct 1 hr block	^{111}In-DTPA-Oct 1 hr block	^{111}In-DTPA-Oct 1 hr block
Adrenals	2.86 ± 0.29	0.16 ± 0.12	16.9 ± 1.44	0.45 ± 0.06	1.11 ± 0.22	0.13 ± 06
Pancreas	0.86 ± 0.14	0.15 ± 0.012	0.59 ± 0.04	0.16 ± 0.02	0.42 ± 0.09	0.11 ± 0.02
Tumor	0.91 ± 0.23	0.25 ± 0.03	0.69 ± 0.07	0.24 ± 0.009	0.57 ± 0.10	0.18 ± 0.03

One group of rats per compound received 250 μg octreotide as a block. Data are presented as %ID/g ± s.d.

TABLE 4
Excretion of Copper-64-TETA-D-Phe[1]-Octreotide and Copper-64-CPTA-D-Phe[1]-Octreotide in Sprague-Dawley Rats

	^{64}Cu-TETA-D-Phe[1]-octreotide (n = 8)		^{64}Cu-CPTA-D-Phe[1]-octreotide (n = 10)	
	1 hr	24 hr	1 hr	24 h
Urine	55.5 ± 13	72.7 ± 15.4	6.2 ± 3.8	35.8 ± 4.8
Feces	<0.2	7.77 ± 2.93	<0.2	5.76 ± 1.35

All data are given as % injected dose ± s.d.

has proven to be more sensitive than ^{111}In-labeled 1A3 for detecting small lesions and metastases (*19,29*). Quantitative biodistribution of patients with colorectal cancer has also been accomplished with PET imaging following injection of ^{64}Cu-labeled MAb 1A3 (*30*).

Synthesis of Octreotide Conjugates

The conjugates TETA-D-Phe[1]-octreotide and CPTA-D-Phe[1]-octreotide were prepared by solution phase synthesis starting with commercially available octreotide. The ε-amino group of Lys on octreotide was blocked with the Boc group to allow selective conjugation of the bifunctional chelate onto the N-terminal amine. N-ε-Boc-Lys[5]-octreotide was prepared in 60%–70% yield and was then purified by RP-HPLC prior to conjugation; the other major product (30%–40%) was N-ε-Boc-Lys[5]-N-α-Boc-D-Phe[1]-octreotide. The bifunctional chelate octreotide conjugates were also purified by RP-HPLC prior to deprotection with TFA. Partially because of the two HPLC purification steps, the syntheses of TETA-D-Phe[1]-octreotide and CPTA-D-Phe[1]-octreotide were time-consuming and the overall yields were low (<5%). A method has been recently developed to synthesize bifunctional chelate octreotide conjugates by solid-phase techniques (*23*). The solid-phase method would be more convenient than the solution phase procedures since there is no need for HPLC purification of intermediate products.

In Vitro Studies

The present study shows that all three radiolabeled octreotide analogs bind to a single class of high affinity somatostatin receptor sites in AtT20 tumor cell membranes, and that both ^{64}Cu-TETA-D-Phe[1]-octreotide (K_d = 314 p*M*) and ^{64}Cu-CPTA-D-Phe[1]-octreotide (K_d = 78 p*M*) bind to the somatostatin receptor with higher affinity than ^{111}In-DTPA-D-Phe[1]-octreotide (K_d = 3.28 n*M*). The somatostatin receptor binding of both ^{64}Cu-labeled octreotide analogs was in the picomolar range, but the receptor binding of ^{64}Cu-CPTA-D-Phe[1]-octreotide was almost five times greater than that of ^{64}Cu-TETA-D-Phe[1]-octreotide. The greater lipophilicity, and smaller size of CPTA versus TETA may be partially responsible for the greater binding affinity of ^{64}Cu-CPTA-D-Phe[1]-octreotide to AtT20 membranes. The binding capacity determined from the Scatchard analysis (B_{max} values) were similar for all radiolabeled octreotide analogs investigated, but the B_{max} determined in this study is about an order of magnitude less than reported by Srikant and Heisler, who found a B_{max} of 1.28 ± 0.1 pmol/mg protein for AtT20 membranes in the determination of the binding affinity of [^{125}I-Tyr[11]]SS-14 (*31*). The differences in the number of receptors determined in the two studies could be partially explained by the difference in AtT20 membrane preparations. The binding capacity of intact AtT20 cells is nearly an order of magnitude lower than that of membranes (0.14 pmole/mg protein) because of the lower number of receptors in the intracellular proteins (*32*). The procedure for preparing membranes in this study may have not sufficiently removed intracellular proteins which contain fewer somatostatin receptors.

Animal Biodistribution Studies

Another radiolabeled octreotide analog for PET imaging of somatostatin receptors, ^{68}Ga[DFO]-octreotide, has been developed by Smith-Jones and colleagues (*17*). Biodistribution of ^{68}Ga[DFO]-octreotide at 1 hr postinjection was similar to that of ^{111}In-DTPA-D-Phe[1]-octreotide in that there was low hepatobiliary clearance, and the major clearance organ was the kidney. A ^{18}F-labeled octreotide, ((2-[^{18}F]Fluoropropionyl-(D)Phe[1])-octreotide) analog has been evaluated in normal mice (*18*). The clearance of this ^{18}F-octreotide analog was primarily through the hepatobiliary system, while the uptake in the adrenals and pancreas decreased steadily up to 1 hr postinjection. The 68-min half-life of ^{68}Ga limits the potential PET imaging time to within the first 2–3 hr postinjection and at these early imaging times it is questionable whether the target-to-nontarget ratios will be great enough for sufficient contrast in PET imaging. Although ^{18}F-octreotide would allow imaging up to 4–6 hr postinjection, there are similar questions concerning clearance of radioactivity from nontarget organs. In our studies with ^{64}Cu-labeled octreotide analogs, we have prepared two ^{64}Cu-labeled octreotide analogs that both show higher binding affinity than ^{111}In-DTPA-D-Phe[1]-octreotide and specific uptake in both normal target organs containing somatostatin receptors and tumors. Also, the longer half-life of ^{64}Cu permits imaging up to 24–36 hr postinjection, which affords potential for better contrast which is important in imaging small metastases.

Tumor-bearing animal models have been used to evaluate somatostatin receptor-based imaging agents. Iodine-123-Tyr-3-octreotide, ^{111}In-DTPA-D-Phe[1]-octreotide and ^{111}In-DTPA-D-Phe[1]-RC-160 (another cyclic peptide somatostatin receptor ligand) were tested in rats bearing somatostatin positive rat pancreatic carcinoma CA20948 (*16,33,34*). In the ^{68}Ga-octreotide study (*17*), receptor-positive tumors in a male Lewis rat were also used, but only the tumor was removed in the biodistribution, not the receptor-rich normal tissues, adrenals and pancreas. In the ^{18}F-octreotide study (*18*), normal mice were utilized in biodistribution experiments and the receptor-rich tissues, adrenals and pancreas were removed. In neither of these

TABLE 5
Comparison of Uptake of Various Radiolabeled Octreotide Analogs in Rodent Models 1 Hour Postinjection

Octreotide analog	Adrenals	Pancreas	Tumor	Reference
^{18}F	0.046	0.056	—	18
^{68}Ga-DFO	—	—	0.095	17
^{111}In-DTPA	0.266 (0.094)	0.101 (0.026)	0.137 (0.043)	this work
^{64}Cu-TETA	0.684 (0.038)	0.206 (0.036)	0.218 (0.060)	this work
^{64}Cu-CPTA	4.06 (0.11)	0.142 (0.038)	0.166 (0.058)	this work

Data are presented as %ID · kg/g body weight. Values in parentheses are nonspecific binding.

cases was the binding demonstrated to be receptor-mediated by administering a blocking dose of a somatostatin analog. In this study, ^{64}Cu-TETA-D-Phe^1-octreotide, ^{64}Cu-CPTA-D-Phe^1-octreotide and ^{111}In-DTPA-D-Phe^1-octreotide were evaluated in normal Sprague-Dawley rats and Lewis rats bearing CA20948 tumors. The tumor, pancreatic and adrenal uptake of all three radiolabeled octreotide analogs are reported in Table 3, and for all analogs the uptake was blocked by coinjection of 250 μg octreotide 1 hr postinjection, indicating receptor-mediated uptake in these tissues. It is possible to compare these data by converting the percent ID per gram to percent ID per kilogram per gram (%ID-kg/g) body weight presented in Table 5. This shows that the uptake of the ^{18}F-octreotide analog in the adrenal and pancreas is only in the range of the nonspecific binding determined in our studies. The tumor uptake obtained with the ^{68}Ga-octreotide analog is lower than that obtained both by the ^{64}Cu-octreotide analogs and ^{111}In-DTPA-D-Phe^1-octreotide. The greater bulk and different charge of the DFO bifunctional chelate compared to DTPA is likely to be responsible for this difference. At the 1 hr time point, both ^{64}Cu-labeled octreotide analogs appear to have superior target tissue uptake than either the ^{68}Ga or ^{18}F analogs.

The high uptake of ^{64}Cu-CPTA-D-Phe^1-octreotide in the adrenals is interesting in that it does not correspond with high tumor or pancreatic uptake. Aguilera et al. (*35*) studied the uptake of ^{125}I-Tyr-somatostatin in male Sprague-Dawley rats. They showed immediate high uptake of iodinated somatostatin in the adrenal capsule with washout occurring after ten minutes. Octreotide was developed due to the rapid metabolism of somatostatin so this washout for labeled somatostatin is not surprising. Although the results of Aguilera et al. are expressed in disintergrations per million per milligram wet tissue, they can be converted into percent injected dose per gram, and a value of 38% ID/g in the adrenal capsule was observed 2–10 min postinjection. Lower values are obtained in the decapsulated adrenal. These investigators do not report pancreatic uptake. The very high uptake that we observed in the adrenals parallels that observed by these workers. In their study, Aguilera et al. showed a specific-to-nonspecific binding ratio of 42.5 in the adrenal capsule. Our ratio for ^{64}Cu-CPTA-D-Phe^1-octreotide in the whole adrenal was 37.5 at 1 hr. Copper-64-CPTA-D-Phe^1-octreotide is therefore not the only somatostatin analog to show this tremendously high adrenal uptake.

In this work, we report the uptake of ^{64}Cu-TETA-D-Phe^1-octreotide, ^{64}Cu-CPTA-D-Phe^1-octreotide and ^{111}In-DTPA-D-Phe^1-octreotide in implanted tumors and in normal somatostatin receptor-containing tissue. Although tumor models have generally been utilized to determine the receptor binding of octreotide (*16,18,33,34*), animal models for the evaluation of other tumor receptors have usually involved uptake in receptor-rich normal tissue. The immature rat uterus has been the target tissue for the evaluation of the estrogen receptor (*36*), the estrogen primed immature rat uterus, which is the model for the progestin receptor (*37*), and the male rat prostate for the androgen receptor (*38*). The relative merits of tumors and normal tissue for the evaluation of estrogen receptors have been discussed (*39*). For both the estrogen receptor ligands (*40,41*) as well as ^{99m}Tc-labeled neogalactosyl albumin (*42*), in vivo situations have been observed where the receptor uptake is flow-limited. In these situations, receptor ligands of very different binding affinity have exactly the same uptake due to the fact that at high organ blood flow, virtually all of the receptor binding ligands are extracted in a single pass. Both the adrenals (*43*) and pancreas (*44*) are regarded as "high flow" organs with blood flow greater than 400 ml per 100 g of tissue per minute. High amounts of receptor ligand should therefore be delivered to both organs. The pancreas, however, has highly vascularized and nonvascularized areas where the adrenals are highly vascularized organs. Differences in blood flow to the different areas of these organs may account for the variations in ligand uptake.

Katzenellenbogen et al. (*40,41*) have discussed in detail the advantages and disadvantages of utilizing high and intermediate receptor rich tissues in animal models. In this study, a comparison of uptake of ^{64}Cu-TETA-D-Phe^1-octreotide and ^{111}In-DTPA-D-Phe^1-octreotide in the pancreas, adrenals and tumors shows that the uptake of ^{64}Cu-TETA-D-Phe^1-octreotide is approximately twice that of ^{111}In-DTPA-D-Phe^1-octreotide in all three organs at 1 hr postinjection. Copper-64-CPTA-D-Phe^1-octreotide has intermediate uptake in the pancreas and tumor but tremendously high uptake in the adrenals compared to the other octreotide analogs. In rats, the adrenals have similar concentrations of somatostatin receptors to the pancreas (*45*). The literature is, however, confusing on the differences in subtypes of somatostatin receptors in these organs (*21,46*). Five different somatostatin receptor subtypes have been cloned (*47–53*) and two ligands (SS-14 and SS-28) have been used to differentiate subtypes (*21*). Srikant and Patel (*21*) have shown different numbers of sites for the binding of SS-14 (B_{max} = 0.35 pmole/mg protein) and SS-28 (B_{max} = 0.205 pmole/mg protein) of the two ligands in the rat adrenal cortex. Thermos et al. (*54*) have shown that in the pancreas, beta-cells predominantly express an SS-28

preferring receptor whereas alpha-cells of the islet have a higher density of SS-14 binding sites. Srikant and Patel (*55*) have studied isolated rat pancreatic acinar cells and have shown a high affinity binding site for the SS-14 ligand in these cells. Srikant et al. (*21*) have investigated binding sites in the pituitary tumor line AtT20. Their data suggests that the receptor exhibits molecular heterogeneity in these tumor cells. The literature data therefore make it difficult to assess whether or not the very high uptake of ^{64}Cu-CTPA-D-Phe^{1}-octreotide in the adrenals is due to differential binding to one of the receptor subtypes. It is, however, interesting that the different target tissues have very different specificity for these somatostatin binding receptor ligands and it is not possible to predict which number can be extrapolated to uptake in a human somatostatin rich tumor.

A possible advantage of ^{111}In-DTPA-D-Phe^{1}-octreotide over the ^{64}Cu-labeled octreotide analogs was the higher absolute tumor uptake and higher tumor-to-nontarget organ ratios at 24 hr postinjection. Indium-111-DTPA-D-Phe^{1}-octreotide did not clear from the tumor as rapidly, and the blood, muscle and liver ^{111}In-DTPA-D-Phe^{1}-octreotide activity decreased to a much greater extent over that of the ^{64}Cu-labeled octreotide analogs. The most favorable tumor-to-nontarget organ ratios for ^{64}Cu-TETA-D-Phe^{1}-octreotide are at 6 hr postinjection (data not shown), suggesting that the optimal time for clinical imaging of ^{64}Cu-TETA-D-Phe^{1}-octreotide may be between 6 and 24 hr postinjection.

The differences in nontarget organ uptake between ^{64}Cu-TETA-D-Phe^{1}-octreotide and ^{64}Cu-CPTA-D-Phe^{1}-octreotide were most likely due to the different lipophilicities of the bifunctional chelates. Copper-64-CPTA-D-Phe^{1}-octreotide cleared primarily through the hepatobiliary system, possibly because of the higher lipophilicity of CPTA. At the later time points, the intestinal uptake of ^{64}Cu-CPTA-D-Phe^{1}-octreotide was also significantly higher than that of ^{64}Cu-TETA-D-Phe^{1}-octreotide or ^{111}In-DTPA-D-Phe^{1}-octreotide ($p < 0.005$). The fecal excretion of ^{64}Cu-CPTA-D-Phe^{1}-octreotide and ^{64}Cu-TETA-D-Phe^{1}-octreotide were not significantly different, which is surprising given the extent of hepatobiliary clearance of ^{64}Cu-CPTA-D-Phe^{1}-octreotide. The intestinal uptake of ^{64}Cu-CPTA-D-Phe^{1}-octreotide increased approximately 40%, from 1 to 24 hr postinjection, while the liver uptake decreased about 40%, indicating that this compound was cleared slowly through the hepatobiliary system. It is likely that ^{64}Cu-CPTA-D-Phe^{1}-octreotide had not significantly cleared by 24 hr postinjection and the activity accumulated in the intestines. The biodistribution of ^{64}Cu-TETA-D-Phe^{1}-octreotide bore a greater similarity to ^{111}In-DTPA-D-Phe^{1}-octreotide, in that the clearance was primarily through the kidneys and more than 50% was excreted into the urine by 1 hr postinjection. There were, however, significant differences between ^{64}Cu-TETA-D-Phe^{1}-octreotide and ^{111}In-DTPA-D-Phe^{1}-octreotide clearance in the kidney. As in the tumor, the concentration of ^{111}In-DTPA-D-Phe^{1}-octreotide in the kidneys remained similar from 1 to 24 hr, whereas ^{64}Cu-TETA-D-Phe^{1}-octreotide cleared over the same time period. The differences in tumor and kidney clearance between ^{64}Cu-TETA-D-Phe^{1}-octreotide and ^{111}In-DTPA-D-Phe^{1}-octreotide are not totally understood, but they might be related to stability of the metal-chelate complex. Possibly the ^{111}In is released from the DTPA chelate in the tumor or kidney cells and trapped by intracellular proteins. Studies on the metabolism of metal-bifunctional chelate-octreotide conjugates would be useful in determining the metabolic product in both target and nontarget organs to design better radiolabeled octreotide conjugates.

Copper-64 also has potential as a therapeutic radionuclide. Apelgot et al. (*56*) reported that ^{64}Cu and ^{67}Cu have similar lethal efficiency in damaging DNA in tumor cells. Our group at Washington University has confirmed their results in LS174T colon cancer cells (*57*), and in tumor-bearing hamsters, ^{64}Cu-labeled MAb 1A3 was shown to inhibit growth of GW39 human colon cancer tumors for longer than 5 mo (*56*). Studies are in progress to evaluate ^{64}Cu-labeled octreotide analogs as potential radiotherapeutic agents. A radionuclide with PET and therapeutic capabilities such as ^{64}Cu could be very advantageous, because accurate individualized dosimetry could be obtained on each patient using PET imaging prior to radiotherapy.

CONCLUSION

This article describes the development of two new ^{64}Cu-labeled octreotide analogs for PET imaging and potential radiotherapy of somatostatin receptor-positive tumors. These new agents have been directly compared to ^{111}In-DTPA-D-Phe^{1}-octreotide both in vitro and in vivo. Both ^{64}Cu-labeled octreotide analogs have higher affinity for the somatostatin receptor in AtT20 mouse pituitary carcinoma cell membranes and have specific uptake in target tissues as great or greater than ^{111}In-DTPA-D-Phe^{1}-octreotide. Although both ^{64}Cu-labeled octreotide analogs contain a macrocyclic bifunctional chelate that is a derivative of cyclam, their biological clearances are entirely different. Copper-64-TETA-D-Phe^{1}-octreotide has a more favorable renal clearance similar to ^{111}In-DTPA-D-Phe^{1}-octreotide and will be invesigated clinically as a PET imaging agent for somatostatin receptor-positive tumors.

ACKNOWLEDGMENTS

The authors thank Kurt R. Zinn, DVM, PhD for production of ^{64}Cu, Margaret Lanahan, MS for quality control of radiolabeled octreotide analogs, Michael Cristel, MS for helpful discussions on the Scatchard analyses and Gregory A. Grant, PhD for mass spectral data. The authors also thank Gregg B. Fields, PhD and Cynthia G. Fields, MS for their expert advice in the peptide synthesis aspects of the project. This work was supported by National Institutes of Health grant CA64475, U.S. Department of Energy grant DE-FG02-87-ER60512 and Mallinckrodt Medical, Inc.

REFERENCES

1. Guillemin R. Peptides in the brain: the new endocrinology of the neuron. *Science* 1978;202:390–402.
2. Reichlin S. Somatostatin (part 1). *N Engl J Med* 1983;309:1495–1501.
3. Reichlin S. Somatostatin (part 2). *N Engl J Med* 1983;309:1556–1563.
4. Reubi JC, Kvols LK, Krenning EP, Lamberts SWJ. Distribution of somatostatin receptors in normal and tumor tissue. *Metabolism* 1990;39:(suppl 2):78–81.
5. Reubi JC, Heitz PU, Landolt AM. Visualization of somatostatin receptors and correlation with immunoreactive GH and PRL in human pituitary adenomas: evidence for different tumor subclasses. *J Clin Endocrinol* 1987; 65:65–73.
6. Reubi JC, Kvols LK, Waser B, et al. Detection of somatostatin receptors in surgical and percutaneous needle biopsy samples of carcinoids and islet cell carcinomas. *Cancer Res* 1990;50:5959–5977.
7. Reubi JC, Maurer R, Klijn JGM, et al. High incidence of somatostatin receptors in human meningiomas: biochemical characterization. *J Clin Endocrinol* 1986;63:433–438.
8. Reubi JC, Waser B, Foekens JA, Klijn JGM, Lamberts SWJ, Laissue J. Somatostatin receptor incidence and distribution in breast cancer using receptor autoradiography: relationship to EGF-receptors. *Int J Cancer* 1990; 46:416–420.
9. Fekete M, Wittliff JL, Schally AV. Characteristics and distribution of receptors for [D-Trp^6]-luteinizing-hormone-releasing hormone, somatostatin, epidermal growth factor and sex steroids in 500 biopsy samples of human breast cancer. *J Clin Lab Anal* 1989;3:137–141.
10. Reubi JC, Waser B, Sheppard M, Macaulay V. Somatostatin receptors are present in small-cell by not in non-small-cell primary lung carcinomas: relationship to EGF receptors. *Int J Cancer* 1990;45:269–274.
11. Bauer W, Briner U, Doepfner W, et al. SMS 201-995: a very potent and selective octapeptide analogue of somatostatin with prolonged action. *Life Sci* 1982;31:1133–1140.
12. Lamberts SWJ, Bakker WH, Reubi JC, Krenning EP. Somatostatin receptor imaging in vivo localization of tumors with a radiolabeled somatostatin analog. *J Steroid Biochem Mol Biol* 1990;37:1079–1082.
13. Bakker WH, Albert R, Bruns C, et al. [^{111}In-DTPA-D-Phe^1]-octreotide, a potential radiopharmaceutical for imaging of somatostatin receptor-positive tumors: synthesis, radiolabeling and in vitro validation. *Life Sci* 1991;49: 1583–1591.
14. Bakker WH, Krenning EP, Breeman WA et al. In vivo use of radioiodinated somatostatin analogue: dynamics, metabolism and binding to somatostatin receptor-positive tumors in man. *J Nucl Med* 1991;32:1184–1189.
15. Krenning EP, Bakker WH, Kooij PPM, et al. Somatostatin receptor scintigraphy with indium-111-DTPA-D-phe^1-octreotide in man: metabolism, dosimetry and comparison with iodine-123-Tyr-octreotide. *J Nucl Med* 1992; 33:652–658.
16. Bakker WH, Krenning EP, Reubi JC, et al. In vivo application of [^{111}In-DTPA-D-Phe^1]-octreotide for detection of somatostatin receptor-positive tumors in rats. *Life Sci* 1991;49:1593–1601.
17. Smith-Jones PM, Stolz B, Bruns C, et al. Gallium-67/gallium-68-[DFO]-octreotide-a potential radiopharmaceutical for PET imaging of somatostatin receptor-positive tumors: synthesis and radiolabeling in vitro and preliminary in vivo studies. *J Nucl Med* 1994;35:317–325.
18. Guhlke S, Wester H-J, Bruns C, Stöcklin G. (2-[^{18}F]Fluoropropionyl-(D)-phe^1)-octreotide, a potential radiopharmaceutical for quantitative somatostatin receptor imaging with PET: synthesis, radiolabeling, in vitro validation and biodistribution in mice. *Nucl Med Biol* 1994;21:819–825.
19. Philpott GW, Schwarz SW, Anderson CJ, et al. RadioimmunoPET: detection of colorectal carcinoma with positron-emitting copper-64-labeled monoclonal antibody. *J Nucl Med* 1995;36:1818–1824.
20. Maurer R, Reubi JC. Somatostatin receptors in the adrenal. *Mol Cell Endocrinol* 1986;45:81–90.
21. Srikant CB, Patel YC. Somatostatin receptors in the rat adrenal cortex: characterization and comparison with brain and pituitary receptors. *Endocrinology* 1985;116:1717–1723.
22. Studer N, Kaden TA. One-step synthesis of mono-N-substituted azamacrocycles with a carboxylic group in the side-chain, and their complexes with Cu^{2+} and Ni^{2+}. *Helv Chim Acta* 1986;69:2081–2086.
23. Edwards WB, Fields CG, Anderson CJ, Pajeau TS, Welch MJ, Fields GB. Generally applicable, convenient solid-phase synthesis and receptor affinities of octreotide analogs. *J Med Chem* 1994;37:3749–3757.
24. Setyono Han B, Henkelman MS, Fockens JA, Klijn JGM. Direct inhibitory effects of somatostatin (analogues) on the growth of human breast cancer cells. *Cancer Res* 1987;47:1566–1570.
25. Munson PJ, Rodbard D. LIGAND: a versatile computerized approach for characterization of ligand binding systems. *Anal Biochem* 1980;107:220–239.
26. Reubi JC, Horisberger U, Essed CE, Jeekel J, Klijn JGM, Lamberts SWJ. Absence of somatostatin receptors in human exocrine pancreatic adenocarcinomas. *Gastroenterology* 1988;95:760–763.
27. Thermos K, Reisine T. Somatostatin receptor subtypes in the clonal anterior pituitary cells lines AtT20 and GH3. *Mol Pharm* 1988;33:370–377.
28. Axelrod J, Reisine T. Stress hormones: their interaction and regulation. *Science* 1984;224:452–459.
29. Philpott GW, Dehdashti F, Schwarz SW, et al. Positron emission tomography (PET) with Cu-64-labeled monoclonal antibody (MAb 1A3) in colorectal cancer [Abstract]. *J Nucl Med* 1994;35(suppl):12P.
30. Cutler PD, Schwarz SW, Anderson CJ, et al. Dosimetry of ^{64}Cu-labeled monoclonal antibody 1A3 as determined by PET imaging of the torso. *J Nucl Med* 1995;36:2363–2371
31. Srikant CB, Heisler S. Relationship between receptor binding and biopotency of somatostatin-14 and somatostatin-28 in mouse pituitary tumor cells. *Endocrinology* 1985;117:271–278.
32. Richardson UI, Schonbrunn A. Inhibition of adrenocorticotropin secretion by somatostatin in pituitary cells in culture. *Endocrinology* 1981;108:281–290.
33. Bakker WH, Krenning EP, Breeman WA, et al. Receptor scintigraphy with a radioiodinated somatostatin analogue: radiolabeling, purification, biologic activity and in vivo application in animals. *J Nucl Med* 1990;31:1501–1509.
34. Breeman WAP, Hofland LJ, van der Pluijm M, et al. A new radiolabeled somatostatin analogue [^{111}In-DTPA-D-Phe^1]RC-160: preparation, biological activity, receptor scintigraphy in rats and comparison with [^{111}In-DTPA-D-Phe^1]octreotide. *Eur J Nucl Med* 1994;328–335.
35. Aguilera G, Parker DS, Catt KJ. Characterization of somatostatin receptors in the rat adrenal glomerulosa zone. *Endocrinology* 1982;111:1376–1384.
36. French AN, Napolitano E, Vanbrocklin HF, Hanson RN, Welch MJ, Katzenellenbogen JA. Synthesis, radiolabeling and tissue distribution of 11β-fluoroalkyl- and 11β-fluoroalkoxy-substituted estrogens: target tissue uptake selectivity and defluorination of a homologous series of fluorine-18-labeled estrogens. *Nucl Med Biol* 1993;20:31–47.
37. Pomper MG, Pinney KG, Carlson KE, et al. Target tissue uptake selectivity of three fluorine-substituted progestins: potential imaging agents for receptor-positive breast tumors. *Nucl Med Biol* 1990;17:309–319.
38. Liu A, Dence CS, Welch MJ, Katzenellenbogen JA. Fluorine-18-labeled androgens: radiochemical synthesis and tissue distribution studies on six fluorine-substituted androgens, potential imaging agents for prostatic cancer. *J Nucl Med* 1992;33:724–734.
39. Mathias CJ, Welch MJ, Katzenellenbogen JA, et al. Characterization of the uptake of 16α-([^{18}F]fluoro)-17β-estradiol in DMBA-induced mammary tumors. *Nucl Med Biol* 1987;14:15–25.
40. Katzenellenbogen JA, Mathias CJ, Vanbrocklin HF, Brodack JW, Welch MJ. Titration of the in vivo uptake of 16α-([^{18}F]fluoro)-17β-estradiol by target tissues in the rat: competition by tamoxifen and implications for quantitiating estrogen receptors in vivo and the use of animal models in receptor-binding radiopharmaceutical development. *Nucl Med Biol* 1993;20: 735–745.
41. VanBrocklin HF, Carlson KE, Katzenellenbogen JA, Welch MJ. 16β-([^{18}F]fluoro)estrogens: systematic investigation of a new series of fluorine-18-labeled estrogens as potential imaging agents for estrogen-receptor-positive breast tumors. *J Med Chem* 1993;36:1619–1629.
42. Krohn KA, Vera DR, Stadalnik RC. A complimentary radiopharmaceutical and model for quantitating hepatic binding protein receptors. In: Eckelman WC, ed. *Receptor binding radiotracers*, vol. II, Boca Raton, FL: CRC Press; 1982:41–59.
43. ICRP Publication 53. *Radiation dose to patients from radiopharmaceuticals*. New York: Pergamon Press; 1987.
44. Ruch T, Patton, H. *Physiology and biophysics*, 19th ed. Philadelphia: W.B. Saunders; 1965.
45. Srikant CB, Murthy KK, Escher EE, Patel YC. Photoaffinity labeling of somatostatin receptor: identification of molecular subtypes. *Endocrinology* 1992;130:2937–2946.
46. Srikant CB, Patel YC. Chemical cross-linking of somatostatin receptors in rat adrenal cortex. *Biochem Biophys Res Commun* 1986;139:757–762.
47. Yamada Y, Post SR, Wang K, Tager HS, Bell GI, Seino S. Cloning and functional characterization of a family of human and mouse somatostatin receptors expressed in brain, gastrointestinal tract and kidney. *Proc Natl Acad Sci USA* 1992;89:251–255.
48. Yamada Y, Reisine T, Law FS, et al. Somatostatin receptors, an expanding gene family: cloning and functional characterization of human SSTR3, a protein coupled to adenylyl cyclase. *Mol Endocrinol* 1993;6:2136–2142.
49. Rens-Domiano S, Law SF, Yamada Y, Seino S, Bell GI, Reisine T. Phar-

macological properties of two cloned somatostatin receptors. *Mol Pharmacol* 1992;42:28–34.
50. Raynor K, O'Carroll AM, Kong AM, et al. Characterization of cloned somatostatin receptors SSTR4 and SSTR5. *Mol Pharmacol* 1993;44:385–392.
51. Corness JD, Demchyshyn LL, Seeman P, et al. A human somatostatin receptor (SSTR3) located on chromosome 22 displays preferenctial affinity for somatostatin-14 like peptides. *FEBS Letts* 1993;321:279–284.
52. Demchyshyn LL, Srikant CB, Sunahara RK, et al. Cloning and expression of a human somatostatin-14-selective receptor variant (somatostatin receptor 4) located on chromosome 20. *Mol Pharmacol* 1993;43:894–901.
53. Panetta R, Greenwood MT, Warszynska A, Demchyshyn LL, et al. Molecular cloning, functional characterization, and chromosomal localization of a human somatostatin receptor (somatostatin receptor type 5) with preferential affinity for somatostatin-28. *Mol Pharmacol* 1994;45:417–427.
54. Thermos K, Meglasson MD, Nelson J, Lounsbury KM, Reisine T. Pancreatic beta-cell somatostatin receptors. *Endocrinol Metab* 1990;22:E216–E224.
55. Srikant CB, Patel YC. Somatostatin receptors on rat pancreatic acinar cells. *J Biol Chem* 1986;261:7690–7696.
56. Apelgot S, Coppey J, Gaudemer A, et al. Similar lethal effect in mammalian cells for two radioisotopes of copper with different decay schemes, ^{64}Cu and ^{67}Cu. *Int J Radiat Biol* 1989;55:365–384.
57. Connett JM, Anderson CJ, Baumann ML, et al. Copper-67 and Cu-64-labeled monoclonal antibody (MAb) as potential agents for radioimmunotherapy [Abstract]. *J Nucl Med* 1993;34(suppl):216P.
58. Anderson CJ, Connett JM, Guo LW, et al. Initial comparison of Cu-67 and Cu-64-labeled anticolorectal carcinoma Mab 1A3 as agents for radioimmunotherapy in tumor-bearing hamsters [Abstract]. *J Nucl Med* 1994;35(suppl):161P.